29 p.

SUPPORT SYSTEMS AND EXCITATION TECHNIQUES FOR DYNAMIC MODELS OF SPACE VEHICLE STRUCTURES

Robert W. Herr and Huey D. Carden

NASA Langley Research Center
Langley Station, Hampton, Va.

Presented at the Symposium on Aeroelastic and Dynamic Modeling Technology

Dayton, Ohio,
September 23-25, 1963

SUPPORT SYSTEMS AND EXCITATION TECHNIQUES FOR DYNAMIC MODELS OF SPACE VEHICLE STRUCTURES

Robert W. Herr and Huey D. Carden

NASA Langley Research Center

ABSTRACT

15625

This paper discusses several techniques for supporting and exciting dynamic models of space vehicle structures to study their dynamic properties such as natural frequencies, mode shapes, damping, and response. Particular attention is given to a unique support harness for vertical support of missile-like structures with minimum lateral restraint. Included in the discussion of vibration exciters is an air shaker which is particularly useful for excitation of the natural modes of light structures and those having thin skins such as encountered on dynamic models of space vehicles.

INTRODUCTION

The accurate experimental determination of the free-free lateral vibration modes of launch vehicles is complicated by the fact that during vibration testing, the vehicle must be restrained against gravity. A massless restraint added to the vehicle anywhere other than at a nodal point will increase the natural frequencies. This increase in the natural frequencies is dependent on both the location and the magnitude of the restraint.

Obviously, the ideal location for the restraint is at the nodal points. From a practical standpoint, this is often not feasible; particularly when the vehicle is liquid fueled and must be orientated vertically. In this case, the only part of the structure capable of supporting the mass of the vehicle is usually at the base where the engine thrust is transmitted to the structure.

One of the primary worries of the dynamics engineer is just how much his suspension system is affecting the natural frequencies. In many cases he worries needlessly and in others, he worries too little. One of the objectives of this paper is to give the dynamics engineer some guidelines as to the importance of restraints imposed by various support techniques.

Also of concern to the dynamicist during the testing and experimental investigations is whether the means of applying the desired force to the structure alters or significantly influences the mass and stiffness properties of the structure. That is, does the exciting and measuring apparatus change and distort the quantities he seeks to measure.

In the cases where large, massive, or relatively rigid structures such as full-scale boosters or space vehicles are being tested, the added mass is quite often only a few percent of the local structure mass and its effects can be neglected. Of the many types of large vibration machines utilized for such tests the most commonly used are the electrodynamic and hydraulic. Since the effects of these exciters on larger structures are generally small or can be minimized through the use of flexible couplings and by placement of the attachment point near nodal locations, only brief and limited comments on these machines will be included.

On the other hand, as the size of the structure decreases the problem and headache of distortion and influence on the structure of the exciter becomes, in many instances, so large that the data in these cases are questionable or cannot be obtained. This emphasizes the necessity for using equipment of a scale appropriate to the structure to be tested. This is particularly true for tests on flexible panels, light, thin-walled conical or cylindrical structures, or small dynamic models of space vehicles. Somewhat more detailed discussions of excitation equipment useful in these areas will be indicated with particular attention given to the description, use, and principle of operation of an air-jet shaker.

SUSPENSION SYSTEMS

General

In general, the most convenient type of spring for the restraint of a launch vehicle during lateral vibration testing is the gravity spring. In this type of suspension, the test vehicle is supported by a cable or cables attached to a rigid overhead framework. The direction of vibration excitation is normal to the plane of the cables.

For a replica model of a vehicle and its cable suspension, dynamic similarity is obtained if the ratio of the pendulum to structural frequencies remains constant. Thus,

$$\left(\frac{\omega_p}{\omega}\right)^2 \propto \frac{g/L}{\omega^2} = \frac{g}{\omega^2 L} = C$$

where ω_p is the pendulum frequency; ω, a structural frequency; g, the acceleration; and L, a characteristic length. Since the characteristic frequency of a model which possesses replica proportions is inversely proportional to its size, it follows that $gL = C$. Hence, for a 1/5-scale vehicle and cable suspension, dynamic similarity is achieved only by testing in a 5g gravity field.

Since the objective of scale model vibration tests is not usually to duplicate the results of full-scale shake tests, but rather to determine, as accurately as possible, the free-free vibration frequencies, the logical approach is to conduct the tests in a 1 g gravity field utilizing a suspension system which has a minimum effect on the natural frequencies.

In order to give some insight into the magnitude of the effects of various suspension systems on the free-free frequencies, the resonant frequencies of uniform beams restrained as indicated in figure 1 were determined experimentally and/or calculated and compared with the free-free frequencies. The effects of the parameter $g/\omega_{ff}^2 L$ were also determined by utilizing uniform beams of varying length or stiffness. ω_{ff} is the first free-free frequency in radians per second and L the length of the beam.

The physical significance of the value of $g/\omega_{ff}^2 L$ is not readily apparent. For replica models, $g/\omega_{ff}^2 L$ is proportional to the size of the vehicle. For a given size vehicle, the parameter is proportional to its mass and inversely proportional to its stiffness. With cognizance of the fact that the stiffness and mass distributions of launch vehicles are seldom uniform, the approximate values of $g/\omega_{ff}^2 L$ for some launch vehicles are: Vanguard, 0.0008; Redstone, 0.0011; Saturn SA-1, 0.0011; Titan, 0.0017; and Saturn 5, 0.0020. A proposed version of Nova would have a relatively large value for $g/\omega_{ff}^2 L$ of 0.0045. The uniform beams utilized in the experiments covered the range of $g/\omega_{ff}^2 L$ up to approximately 0.010 which represents an extremely flexible beam.

Perhaps a better feel for the significance of $g/\omega_{ff}^2 L$ is afforded by the fact that for a horizontally supported beam, the static deflection relative to its length is proportional to $g/\omega_{ff}^2 L$. For a horizontal cantilever, the static deflection at the tip divided by the length of the beam is equal to $62.8\left(g/\omega_{ff}^2 L\right)$. Thus, the static deflection curves for horizontal cantilevers would appear as depicted below.

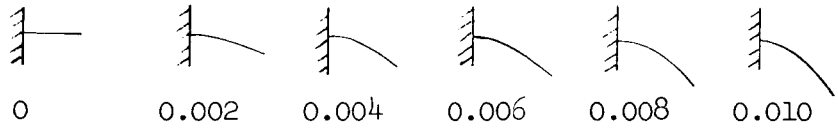

$$\frac{g}{\omega_{ff}^2 L}$$

Two-Cable Horizontal Suspension

If the structure of the vehicle is rugged enough to withstand the bending moments, the suspension system depicted in figure 1(a) is probably the most desirable due to its simplicity. If the support cables are located at nodal points, their effect on the free-free frequencies are negligible.

It is not always feasible to support a vehicle at the nodal points. The increase in the resonant frequency then depends on the location of the support points, the length of the cables, and the value of the parameter $g/\omega_{ff}^2 L$.

In figure 2, the increase in the first natural free-free frequency, indicated by the ratio ω/ω_{ff}, is plotted as a function of the ratio of the distance to the support points from the ends of the beam to the beam length, S/L, for cable lengths of 1/8, 1/4, and 1/2 the length of the beam and for beams having values of $g/\omega_{ff}^2 L$ of 0.00202, 0.00402, and 0.00605. The free-free reference frequency ω_{ff} used in this figure, as well as in all other experimental figures pertaining to uniform beams, is the experimental frequency for a value of S/L of 0.224.

For the range of parameters investigated, the data of figure 2 show that the increase in frequency due to the suspension is approximately proportional to $g/\omega_{ff}^2 L$ and inversely proportional to the cable length l/L.

For the most flexible beam $\left(\frac{g}{\omega_{ff}^2 L} = 0.00605\right)$ supported on short cables ($l/L = 1/8$), the location of the cable attachment points can be as much as 8 percent of the length of the beam from the nodal points without exceeding an error of 1 percent in the measurement of the free-free first natural frequency. For a more practical value of $\frac{g}{\omega_{ff}^2 L} = 0.002$, the short cables may be located anywhere within 14 percent of the length of the beam from the nodal points without exceeding a 1-percent error.

It is therefore apparent that for cable lengths greater than 1/8 the beam length and for practical values of $\frac{g}{\omega_{ff}^2 L} < 0.002$, there is no need to go to great pains to support the beam precisely at the nodal points. Although not shown here, the cable attachment location has even less effect on the higher free-free modes.

Multicable Horizontal Suspension

In cases where it is not feasible to support a vehicle horizontally at two points due to excessive static bending moments or localized stresses, it may be practical to support it on many cables distributed along the length of the beam as indicated in figure 1(b). If an infinite number of cables are assumed, an elastic lateral foundation results, the modulus of which is K. The frequency equation is

$$\omega^2 = \frac{K}{m} + \omega_{ff}^2$$

where

m = total mass of beam

$K = mg/l$

l = length of cables

Substituting the value of K into the frequency equation and rearranging

$$\frac{\omega}{\omega_{ff}} = \sqrt{\left(\frac{g}{\omega_{ff}^2 L}\right)\left(\frac{L}{l}\right) + 1}$$

In figure 3 the increase in frequency ω/ω_{ff} due to the cable restraint is plotted as a function of $g/\omega_{ff}^2 L$ for cable lengths of $l/L = 1/16$, $1/8$, $1/4$, and $1/2$.

As with the two-cable suspension, the data show that the effect on the first free-free frequency is approximately proportional to $g/\omega_{ff}^2 L$ and inversely proportional to the cable length.

For cable lengths greater than $1/8$ of the beam length and for the common range of $\frac{g}{\omega_{ff}^2 L} < 0.002$, the error is less than 1 percent. For corresponding cable lengths and values of $\frac{g}{\omega_{ff}^2 L}$, the error is approximately one-quarter of the error obtained when the beam is supported by a cable at each end.

In order that the tension in the many cables be properly distributed, it is usually advisable to use elastic shock cords in place of relatively inelastic cables. One experimental data point for which elastic shock cords were utilized is shown in figure 3 and it agrees very well with the theoretical result.

One-Cable Vertical Suspension

Other than its simplicity, the one-cable vertical suspension depicted in figure 1(c) has little to offer. As is the case with liquid-fueled launch vehicles, it is frequently necessary to orientate a test vehicle vertically

during vibration tests. It is a rare vehicle, however, that can withstand the rigors of being hung by its nose.

Despite their lack of general usefulness, the effects of the one-cable suspension on the free-free vibration frequencies are interesting; especially when compared to the results utilizing the two-cable vertical suspension illustrated in figure 1(e).

In figure 4(a) the increase in the first free-free frequency ω/ω_{ff} is plotted as a function of cable length L/l for four beams for which the values of $g/\omega_{ff}^2 L$ are 0.00291, 0.00631, 0.0114, and 0.0255.

It should be noted that increasing cable lengths are denoted by decreasing values of L/l so that $L/l = 0$ represents an infinitely long cable or zero lateral restraint.

The most interesting feature of this plot is that when the curves are extrapolated to a value of $L/l = 0$, there is still a substantial increase in the natural frequency over the free-free frequency. This increase in frequency can be attributed to the tension in the beam.

In figure 4(b), the curves of figure 4(a) have been cross-plotted to show the increase in the natural frequency as a function of $g/\omega_{ff}^2 L$ for relative cable lengths l/L of 1/8, 1/4, 1/2, 1, and ∞.

It can be seen that for cable lengths greater than one-quarter the length of the beam, the tension in the beam has a greater effect on the natural frequency than does the cable restraint.

Vertical Orientation With Restraint at Base

An often used type of restraint for shake tests of liquid-fueled launch vehicles is illustrated in figure 1(d). In this system, all of the pitch and lateral restraint is concentrated at the base of the vehicle. Any of several types of restraining springs may be used, such as a series of coil springs spaced around the periphery at the base, pneumatic bags, or a combination of vertical cables to provide lateral restraint and torsion springs to provide pitch restraint.

No matter what type of restraint is used, a minimum spring constant of mgL_{cg}, must be provided in the pitch direction to restrain a vehicle from toppling. L_{cg} as used here is the distance from the base of the vehicle up to its center of gravity.

If a variation in $g/\omega_{ff}^2 L$ is assumed to represent a change in the gravitational field g, acting on a given vehicle, it is seen that the minimum pitch spring restraint required at the base mgL_{cg} is proportional to

$g/\omega_{ff}^2 L$. It is thus apparent that as the gravitational attraction on a given vehicle is increased, the minimum spring restraint must also be increased resulting in a larger effect on the natural frequencies. Similarly, for replica models tested in a constant gravitational field, the greater the size of the vehicle, the greater will be the effect of the minimum spring restraint on the natural frequencies.

The effect that this minimum pitch restraint has on the first free-free frequency has been computed and is presented in figure 5. In this analysis the lateral restraint was assumed to be zero. Although it is realized that these restraints are impractical from an experimental standpoint, the results indicate the absolute minimum increase in the natural frequencies that can be obtained with this type of restraint.

Figure 5 shows that for a uniform beam having a value of $g/\omega_{ff}^2 L$ corresponding to that of Titan (0.002), the minimum pitch restraint mgL_{cg} $\left(\text{denoted by } \omega_p/\omega_{ff} = 0\right)$ increases the first natural frequency by 4 percent; a relatively large increase when compared to the results obtained utilizing horizontal suspensions with reasonable cable lengths.

When the pitch restraint at the base is increased to provide a finite rigid-body pitch frequency (ω_p), the effect on the first flexural frequency can become quite pronounced. Although a ratio of rigid-body frequency to first free-free frequency of 1/5 may intuitively seem like a soft suspension, it is noted that for a value of $\dfrac{g}{\omega_{ff}^2 L} = 0.002$ the increase in frequency amounts to 12 percent.

Two-Cable Vertical Suspension

A method of supporting a launch vehicle in a vertical position with a minimum of rigid-body restraint but yet safe from the standpoint of toppling has been conceived by the senior author and is depicted in figure 6. The weight of the vehicle is carried by two support cables attached to the bottom of the vehicle. Stability is provided by two restraint cables tied between the support cables and the periphery of the vehicle at some point e_1 above the vehicle's center of gravity. This support system has essentially two degrees of freedom in the plane normal to the cables; translation as a pendulum and pitching.

In terms of the dimensions of figure 6, the total pitching moment acting on the vehicle (including the moments due to gravity) can be shown to be

$$\frac{M}{W} = \frac{\theta e\left(\dfrac{a-d}{f} + \dfrac{c-d}{e}\right)}{2\sqrt{\left(\dfrac{b-d}{2e_1}\right)^2 - \theta^2}} - \theta e\left(1 + \frac{e_1}{f}\right)$$

Taking the derivative of the moment expression with respect to θ gives the effective spring constant of the system in pitch.

$$\frac{K}{W} = \frac{dM}{Wd\theta} = \frac{e\left(\frac{a-d}{f} + \frac{c-d}{e}\right)\left(\frac{b-d}{2e_1}\right)^2}{2\left[\left(\frac{b-d}{2e_1}\right)^2 - \theta^2\right]^{3/2}} - e\left(1 + \frac{e_1}{f}\right)$$

Solving the spring constant equation for a when K and θ are set equal to zero results in an expression defining the cable separation necessary to maintain the vehicle in a vertical altitude with zero pitch frequency.

$$a = f\left(\frac{b-d}{e_1} - \frac{c-d}{e}\right) + b = a_0$$

when $a < a_0$, the vehicle will topple a few degrees to a stable position and when $a > a_0$ it will possess a frequency in pitch >0.

Experimental verification of the critical cable separation distance is shown in figure 7. For a given location of the restraining cables e the support cables were progressively separated until the vehicle would just stand erect. Correlation of the experimental results with theory shows excellent agreement.

In figure 8(a), the pitch moments imposed by the harness relative to the unstable gravity moments $\frac{M_{harness}}{mgL_{cg}\theta}$ have been plotted as a function of the angle of tilt for three values of the relative cable separation a/a_0 for each of two restraining cable locations. The center curves in each case is for $a/a_0 = 1$ which results in a zero pitch frequency when $\theta = 0$. When $a/a_0 < 1$ the vehicle will tilt over until the restraining moment imposed by the harness exceeds the moment due to gravity.

The effective spring constant of the harness in pitch relative to the gravity spring $\frac{K_{harness}}{mgL_{cg}}$ has been plotted in figure 8(b) as a function of the angle of tilt. As may be observed, the effective spring is decidedly nonlinear.

In practice, this harness is extremely simple to use. It is not necessary, as it is with many types of suspension systems, to alter the stiffness of the restraint whenever the fuel load is varied over a wide range. The only adjustment that need be made is the support cable separation as the center of gravity changes.

For large liquid-fueled vehicles it may be necessary to distribute the concentrated loads imposed on the structure at the cable attachment points by means of a lightweight truss. Radial loads applied to the structure due to the tension in the restraining cables may be alleviated by replacing the restraining cables with two parallel cables as illustrated in the sketch.

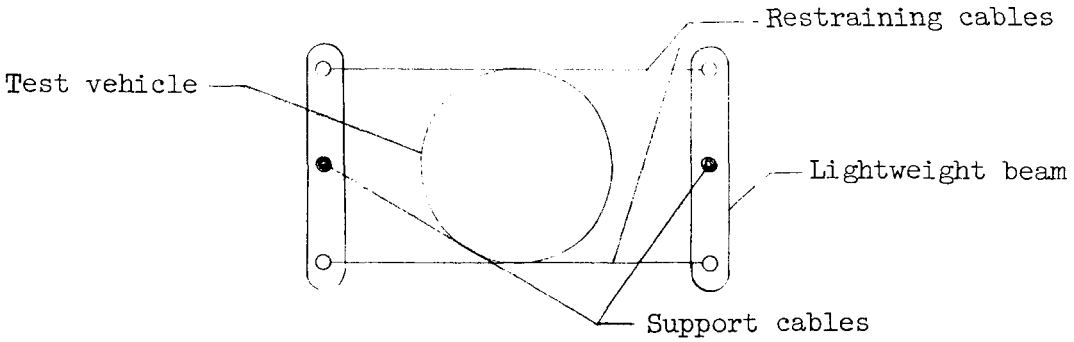

The fact that the rigid-body pitch frequency can be readily adjusted to zero does not imply that the harness has no effect on the free-free frequencies. There is a small amount of lateral restraint at the cable attachment points. In order to establish the effects of these restraints, vibration tests were made of three uniform beams suspended in the harness depicted in figure 9. The effect of the harness on the free-free frequencies will vary with the lengths of the support and restraining cables used but the trends and the magnitude of the effects caused by a particular harness are of interest.

The effects of the location of the restraining cables are indicated in figure 9(a) in which the first natural frequency, relative to the minimum faired frequency, is plotted as a function of restraining cable location l/L. As expected, the location of the restraining cables does have an effect on the natural frequency, but the magnitude of the effect is exceedingly small. For the beam with a value of $\frac{g}{\omega_{ff}^2 L} = 0.002$, the maximum change in frequency attributable to a variation of the restraining cable location is 0.3 percent; a negligible effect.

In figure 9(b), the data to figure 9(a) have been plotted relative to the first free-free frequency. Rather than increasing the natural frequency, as a massless restraint must, the figure shows that natural frequencies of a uniform beam suspended in this harness are appreciably less than the free-free frequencies. Just as tension in a beam increases its flexural frequencies (fig. 4), compression decreases the natural frequencies. Although this effect is small for present-day launch vehicles $\left(\text{perhaps 2 percent at } \frac{g}{\omega_{ff}^2 L} = 0.002\right)$, the important point is that the effects due to the harness restraint are far less, even when the restraining cables are located at the tip of the vehicle.

As mentioned previously, most launch vehicles are not uniform beams. They are, in general, stiffer and more massive at their base resulting in relatively large vibration amplitudes at the tip. Intuitively, it would seem that, compared to a uniform beam, the frequencies of such a vehicle would be affected less by compression due to gravity and relatively more due to a restraint near the tip. In view of such a possibility, the natural frequencies of two nonuniform beams mounted in a harness were obtained and are compared to their free-free frequencies in figure 10. The upper and lower half of each beam was uniform, with the upper half having one-half the mass and one-eighth the stiffness of the lower half. Values of $g/\omega_{ff}^2 L$ for the two beams were 0.002 and 0.006. Although it is not possible to separate experimentally the effects due to restraint and compression, when the results are compared to the uniform beam results of figure 9(b), it can be said that the compression effects are less and/or the restraint effects are greater for the stepped beam. The compression effects still outweigh the restraint effects since the natural frequencies in the harness are lower than the free-free frequencies.

The variation in the natural frequencies associated with a change in location of the restraining cables can be seen to be somewhat greater for the stepped beam than for the uniform beam.

It is not to be implied from these results that the compression effects will in all cases outweigh the restraining effects of the harness.

Although there is no good reason to use a support cable separation greater than the optimum a_0, the results shown in figure 11 indicate that the cable separation is not critical even for an extremely flexible uniform beam. In this figure, the natural frequency is plotted as a function of the cable separation relative to the optimum cable separation a_0. ω_{ref} is the natural frequency obtained with the restraining cables at the nodal point and the support cables separated the optimum distance. The results indicate that when the restraining cables are located at the tip, the effect of increasing the cable separation by 50 percent is about the same order of magnitude as is obtained by moving the restraining cables from the nodal point to the tip.

In figure 12 the effects of the harness type of suspension on the first two free-free frequencies are compared with results obtained when the beams were suspended on one cable attached at the tip as in figure 1(c). The interesting aspect of this figure is the near symmetry of the data about the abscissa. Assuming that tension and compression of uniform beams have equal but opposite effects on the natural frequencies for the range of parameters investigated, the near symmetry of the data indicates a comparatively small effect of the restraint of either suspension system. It is apparent that both suspension systems affect the first free-free frequencies to a much greater extent than the second free-free frequencies. It may also be observed that for the harness suspension, moving the restraining cables from the second mode nodal point to the tip of the beam has an extremely small effect.

With respect to the relatively large increase in frequencies predicted when all of the pitch restraint was applied at the base of the vehicle (fig. 5), it should be noted that these results would have been alleviated

somewhat had compression effects been included in the analysis. It is believed, however, that in this case the compression effects are relatively small compared to the effects attributable to the restraint.

VIBRATION EXCITERS

Electrodynamic Vibration Machines

As the name implies, the electrodynamic vibration machine derives its name from the method of force generation. The force is produced electrodynamically from the interaction between a current flow in a driver coil and the intense magnetic field which cuts the coil.

In utilizing these exciters for exploratory vibration studies, the electrodynamic shaker has the advantages of relatively wide frequency ranges, and availability of random and sinusoidal vibrations or a combination of both. In multiple shaker applications, in-phase and out-of-phase control between the various machines can be accomplished. Although these shakers are versatile and widely used, they have the disadvantage in that it is difficult to provide adequate power and displacement at the low frequencies commonly encountered in large-scale vehicle studies. In their use on smaller scale structures, care must be exercised to minimize the effects of the attachment between the test vehicle and the shaker coil in order to avoid significant influences on the structural responses.

Hydraulic Vibration Machines

The hydraulic vibration machine transforms power in the form of a high-pressure flow of fluid from a pump to a reciprocating motion of the table of the vibration machine. High-pressure fluid delivered to one side of the piston in the actuator and then to the other side, forces the actuator to execute a reciprocating motion.

Some of the disadvantages found in the electrodynamic shaker have been overcome in the hydraulic shaker. For example, the hydraulic shaker is capable of generating large forces and large displacements or strokes at frequencies as low as desired. Relative to the forces attainable, the hydraulic machine is small and lightweight which can be advantageous in certain applications. However, this fact also requires a rigid connection to firm ground or a large massive base to anchor the machine in place which can be inconvenient and difficult in many cases. Among some of the other disadvantages are: secondary resonances, seepage, leakage, nonlinearities, necessity of clean hydraulic fluid, and poor high-frequency performance.

Electromagnetic Vibration Machines

In many applications where the limiting conditions of the other types of vibration testing machines cannot be circumvented, electromagnetic exciters have been successfully utilized. The electromagnetic vibration machine generates a vibratory force which is transmitted to the table, giving it motion;

the force is derived from magnetic attraction or repulsion due to intensity or direction changes of a magnetic flux linking several flux-carrying members.

The simplest form of an electromagnetic vibration exciter, called an unbalanced-force type, consists of an electromagnetic core with a single winding and an armature. Both the core and armature are laminated from magnetic-core material. This simple device, which is generally user-built, has several desirable and useful features. It has been useful in driving structures for resonant mode testing where the structure supplies the position force and where the distortion of the generated force is of little consequence. In these cases, the armature can be bolted or cemented to the test structure at any appropriate location. In the tests for which no addition of mass to the structure can be tolerated, the device can be used without the armature. In these instances, if the structure is magnetic, it acts as the armature and supplies the magnetic circuit. For materials that are conducting but nonmagnetic, eddy currents are generated which produce electrodynamic forces. This shaker is particularly adaptable to the synchronized use of several units for resonant testing of light dynamic wind-tunnel models and the like. Its usable frequency range can easily extend from a few cycles per second to several hundred cycles per second. Among the undesirable features of this exciter are the presence of a large constant attractive force in addition to the vibratory force, and the nonlinearity of the resulting force of the device.

Air-Jet Vibration Exciters

Although our Vibration and Dynamics Laboratory at Langley has a wide variety of electrodynamic and hydraulic shaking equipment, one of the most popular vibration exciters, where low force outputs are sufficient, is the air-jet shaker. As the name implies, an air-jet shaker derives its driving force from the kinetic energy of a stream of high-velocity air, periodically impinging upon the test specimen. Proper modulation of the airflow results in a sinusoidal force output.

The chief assets of the air-jet shaker are that no mass is added to the test specimen and it is extremely simple to use since no mechanical connections to the test specimen are required. Its major liability in the past has been the rapid decrease of force output with increasing frequency. This loss of available force at high frequencies has been due to the internal valving used to modulate the airflow. Most of the potential energy was being wasted in accelerating and decelerating the air column during each cycle.

This problem can be overcome simply by external interruption of the air jet as depicted in figure 13. The stream of high-velocity air which impinges upon the test specimen, exits from the nozzle at a constant velocity and pressure. The airstream is then deflected periodically by a motor-driven notched disk. A nearly sinusoidal force may be obtained by use of a diamond-shaped nozzle, the length of which is equal to the length of the notch in the interrupter disk.

All of the air-jet shakers built in our shop have a single nozzle which results in an unbalanced force. This unbalance is of little consequence for most vibration tests but for some highly damped and flexible test specimens or nonlinear systems it is desirable to have a balanced force input. In such

cases, the air jet may be counterbalanced by directing a steady stream of air onto the opposite side of the test specimen. If the second nozzle has an area equal to one-half the area of the shaker nozzle and is fed from the same pressure line, the net force on the specimen will be closely balanced.

The magnitude of the oscillating force can be controlled by a pressure or flow regulating valve in the air supply line. The maximum peak-to-peak force output when the jet is directed at a large flat plate is approximately 1.3 AP, where A is the area of the nozzle and P the line pressure. The area of the nozzles on present Langley shakers is 0.025 sq in. (0.1-in. × 0.5-in. diamond) which results in a maximum peak-to-peak force of 2.5 pounds when connected to a 100-psi air-supply line. Although this may seem to be a rather small force as vibration exciters go, it has been found to be more than ample to excite the natural modes of panels, thin-wall cylinders, and numerous wind-tunnel models. Since the added mass effects of the air jet are negligible, the driving force may be applied at the point of maximum vibratory amplitude thus transmitting a maximum amount of energy to the test vehicle. The force of a given shaker can be doubled by directing the air jet into a lightweight pelton bucket attached to the test specimen in order to effect a 180° change in the airstream direction.

Larger force outputs may, of course, be obtained by the use of larger nozzles and higher pressure lines but the jet noise soon becomes intolerable and may well distort the output of piezeoelectric-type pickups.

As previously indicated, one of the major shortcomings of the electrodynamic and electromagnetic exciters often encountered is the limited stroke or travel which they impose. The air-jet exciter, in this respect, however, permits very large, unrestrained amplitudes of oscillations. This asset of the air-jet shaker can be illustrated with the aid of figure 14. Shown in the figure is the force coefficient as a function of the plate distance for various size plates, where the force coefficient is the ratio of the force exerted on the plate to the product of nozzle area times the line pressure. The significant point to be made here is that for sufficiently large air-jet impingement areas, there is no appreciable drop in the excitation force even at very large distances. The nozzle used in these experiments was a 0.1-inch × 0.5-inch diamond.

The complexity of the motor-speed control depends upon the use for which the shaker is intended. In applications where accurate control of the frequency is not required, variation of the voltage to an electric motor may be satisfactory. The best all-around speed control that we have tried consists of a small (1/75 hp) synchronous motor driving the interrupter disk through a commercially available variable-speed friction drive. Since the torque required to drive the interrupter disk is very small, there is essentially no slippage in the variable-speed friction drive. The frequency range of our present units covers the range from 0 to 900 cps. A counter, geared to the speed control crank, indicates the frequency directly in cycles per second.

In summing up, it can be said that this type of air-jet shaker exhibits the following assets which make it a valuable tool in dynamic model testing: it is extremely convenient to use since no attachment to the test specimen is required; it is essentially massless; its available force can be calibrated statically and is constant with frequency; the force transmitted to the

structure is independent of frequency and motion of the structure, simplifying control and giving repeatability even with nonlinear structures; and its cost is relatively low.

The chief liabilities of the air-jet shaker are the noise associated with large force outputs and the difficulties encountered in multiple shaker applications.

CONCLUDING REMARKS

In general, the results indicate that when typical launch vehicles are suspended in a horizontal attitude by cables or shock cords, the free-free flexural frequencies are affected very little by the cable restraint when reasonable length cables are utilized. For vertically orientated vehicles where all of the restraint is concentrated at the base, the effect of this restraint on the first natural frequency may become appreciable even when the rigid-body frequencies are very low. Vibration results of vertically orientated beams restrained by a two-cable harness indicate that the effects of the harness restraint on the natural frequencies are small in comparison to the effects of compression in the beam due to gravity.

An air-jet vibration exciter is also described which is easy to use and has a constant force output regardless of frequency. This shaker is particularly useful for vibration testing of small panels, thin-wall cylinders, and lightweight dynamic models where the addition of any mass may have a critical effect on the measured frequencies.

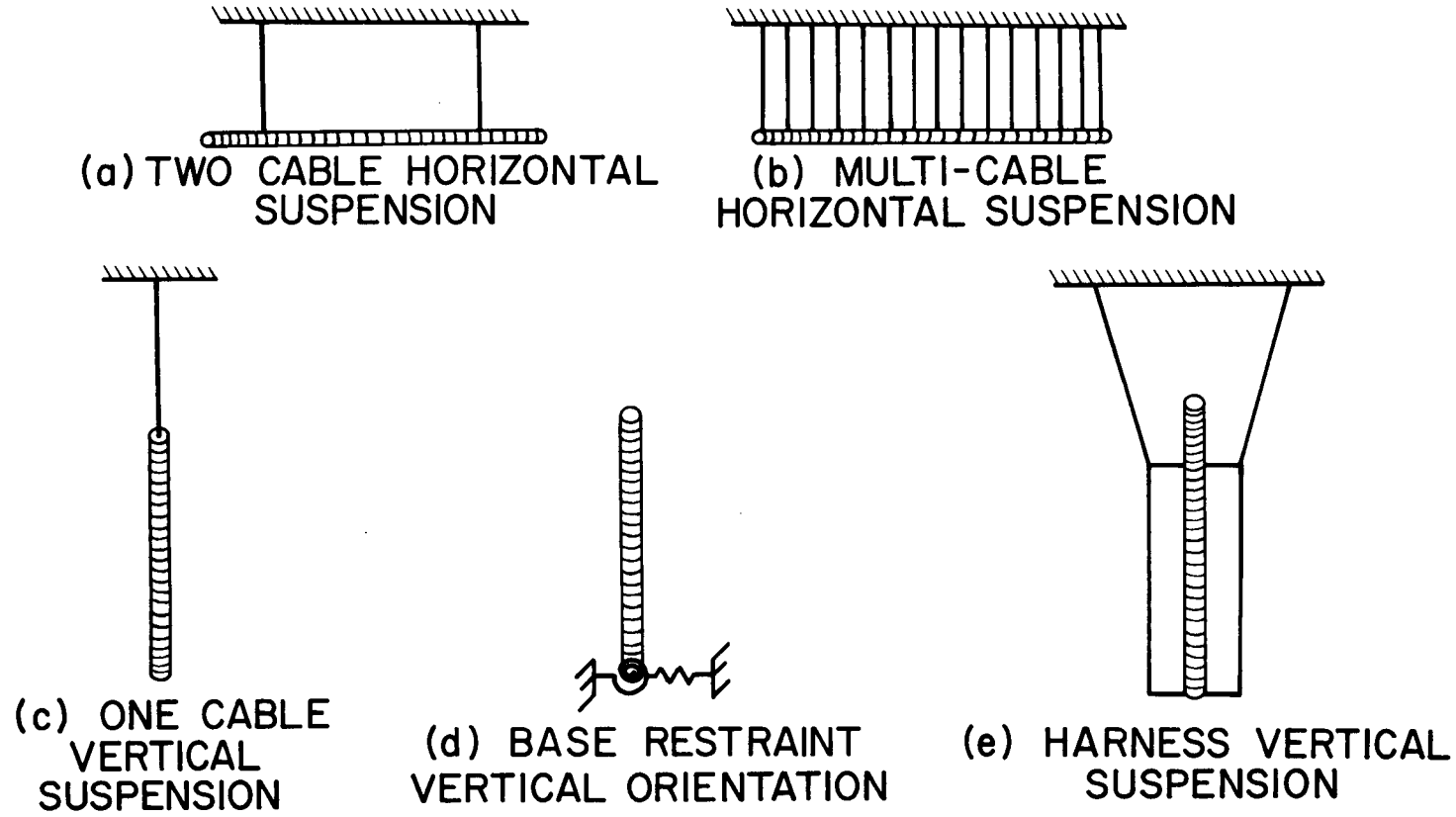

Figure 1.- Types of suspension systems investigated.

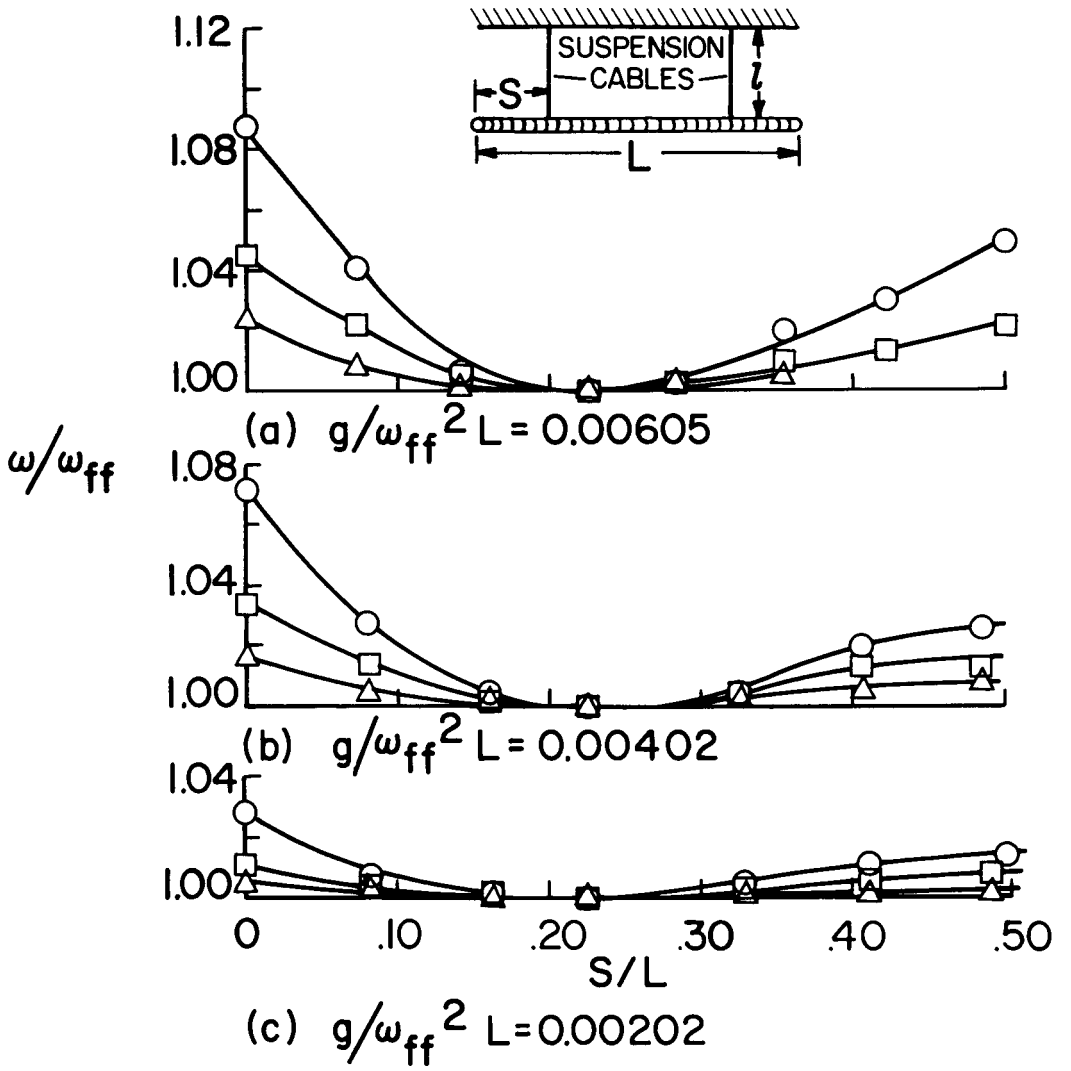

NASA

Figure 2.- Effects of the two-cable horizontal suspension on the first free-free frequency.

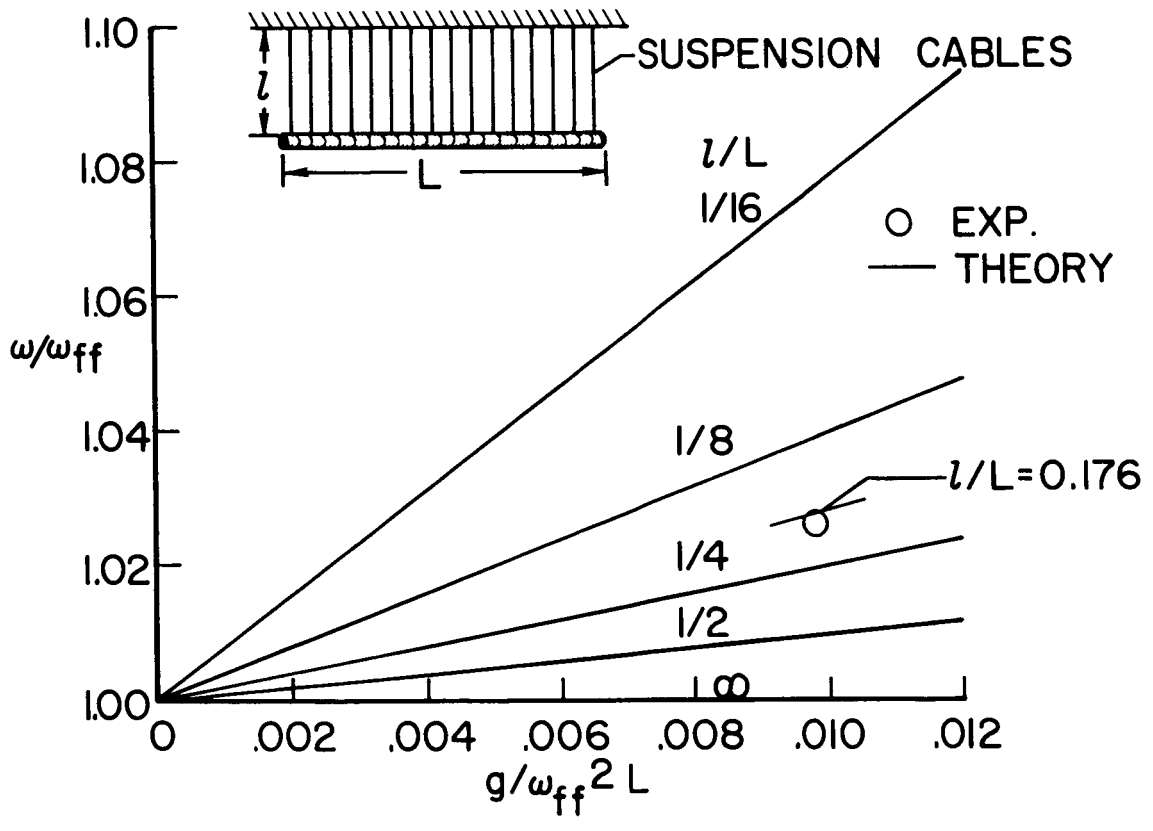

NASA

Figure 3.- Effects of the multicable horizontal suspension on the first free-free frequency.

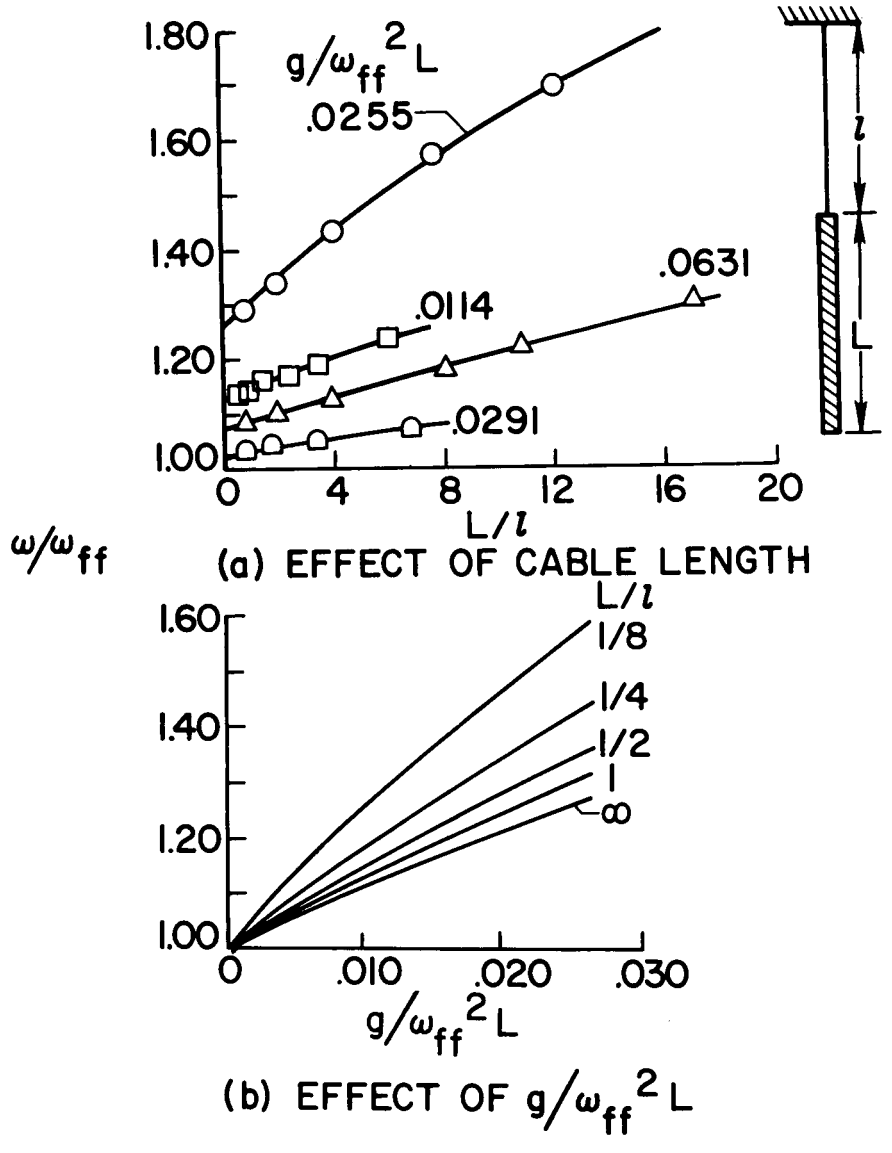

NASA

Figure 4.- Effects of the one-cable vertical suspension on the first free-free frequency.

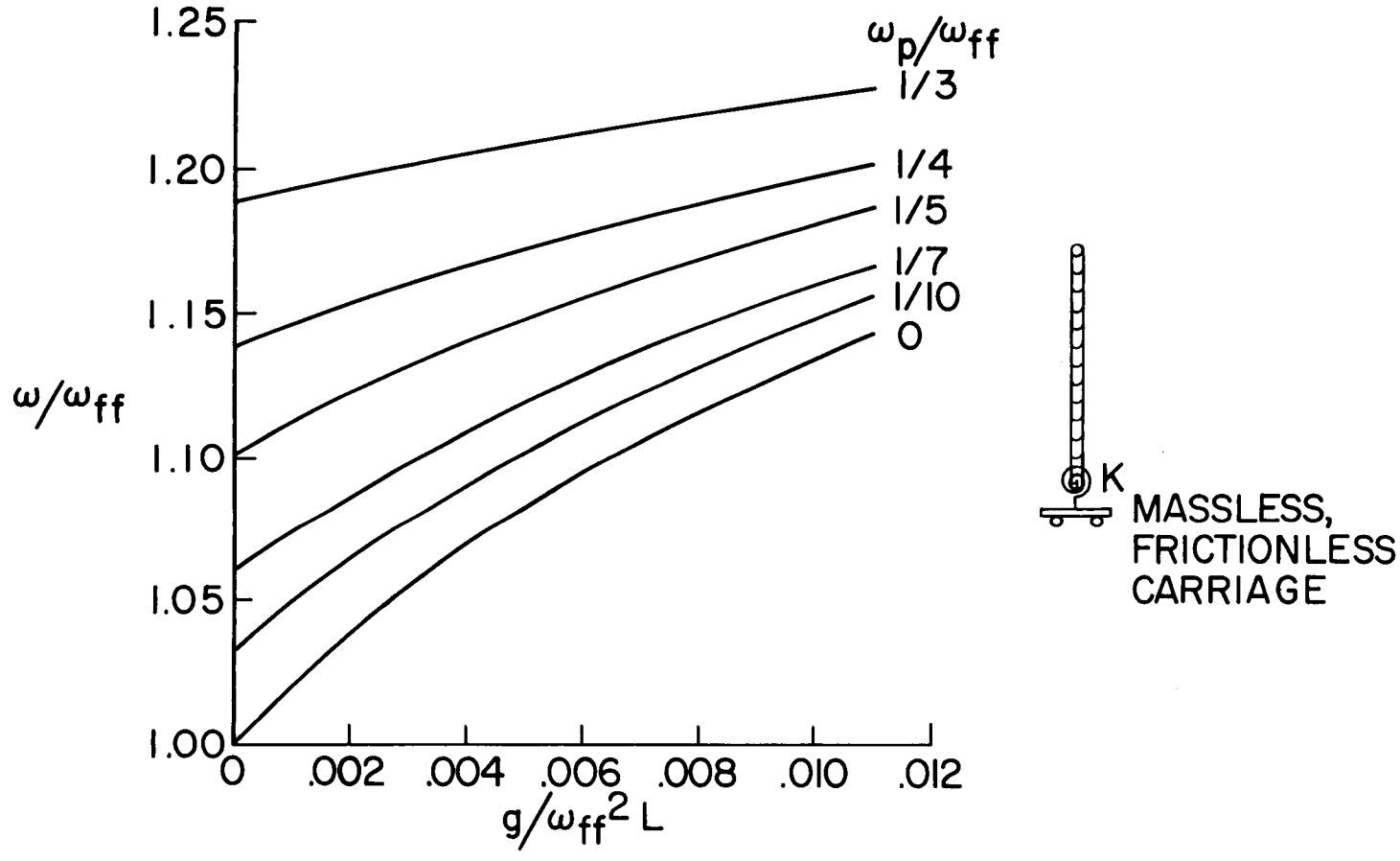

NASA

Figure 5.- Effect on the first free-free frequency of a suspension system having all restraint at the base of the vehicle.

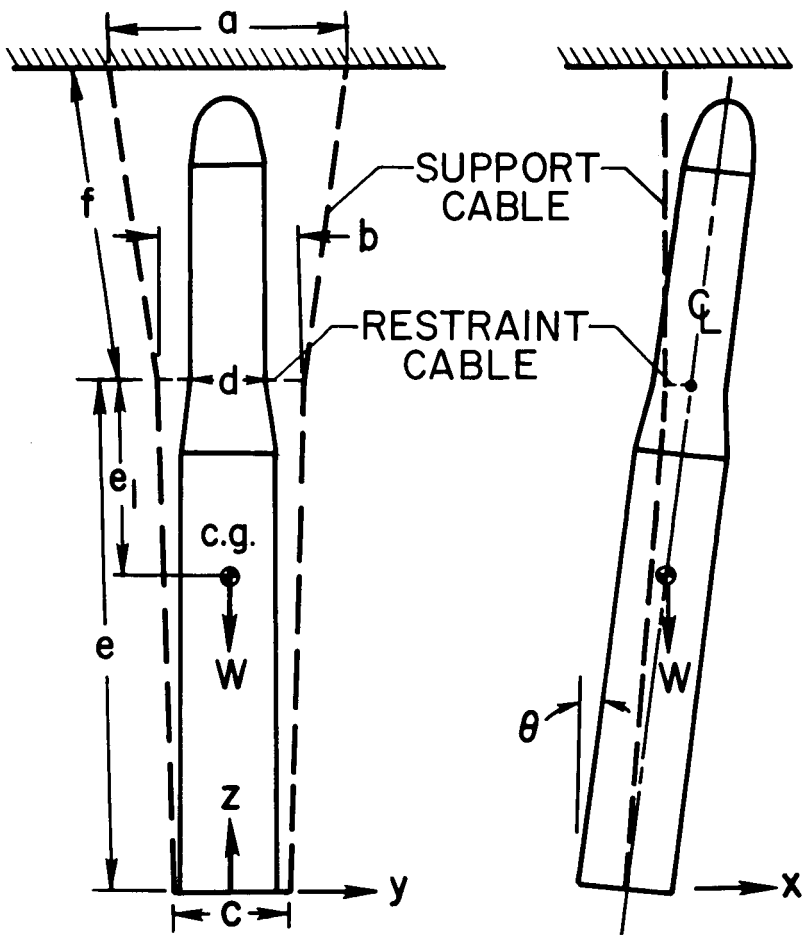

NASA

Figure 6.- Two-cable vertical suspension system.

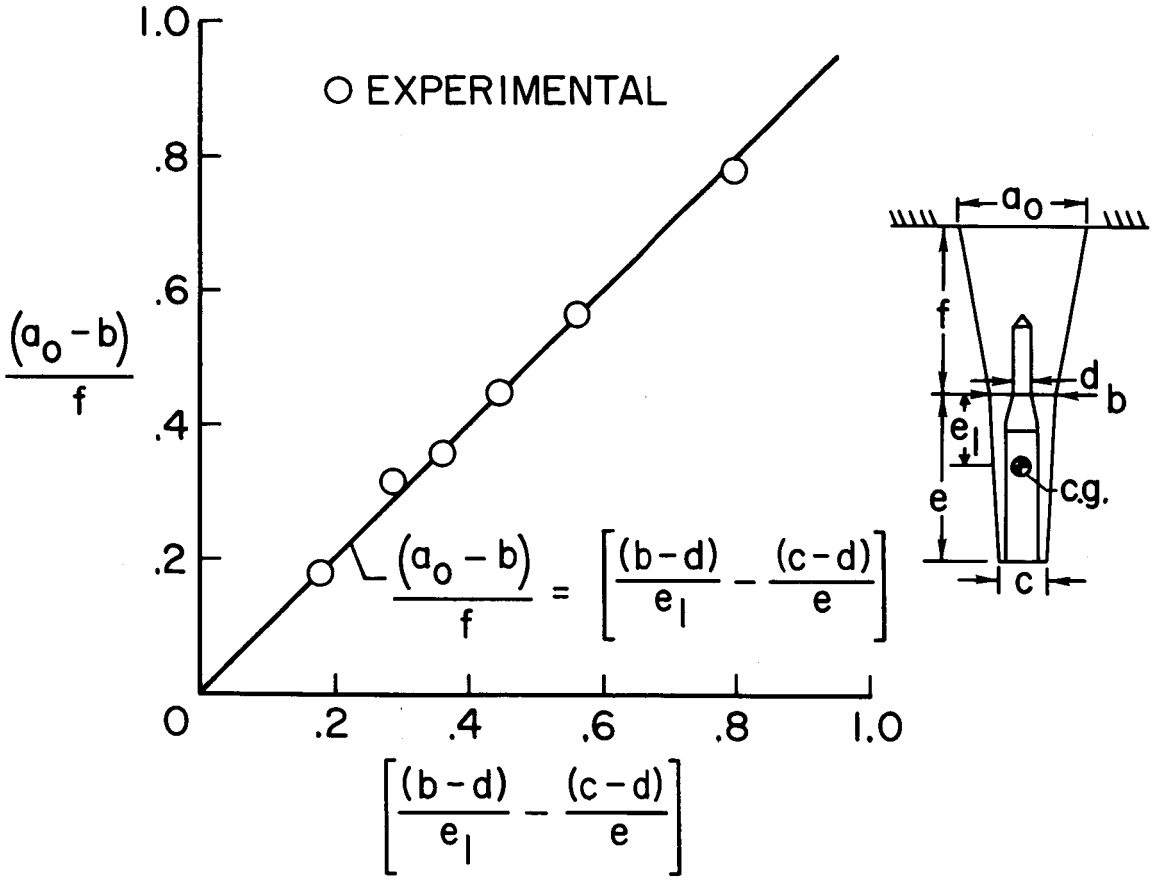

NASA

Figure 7.- Comparison of experimental and calculated values of minimum support-cable separation a_o required to maintain vertical attitude.

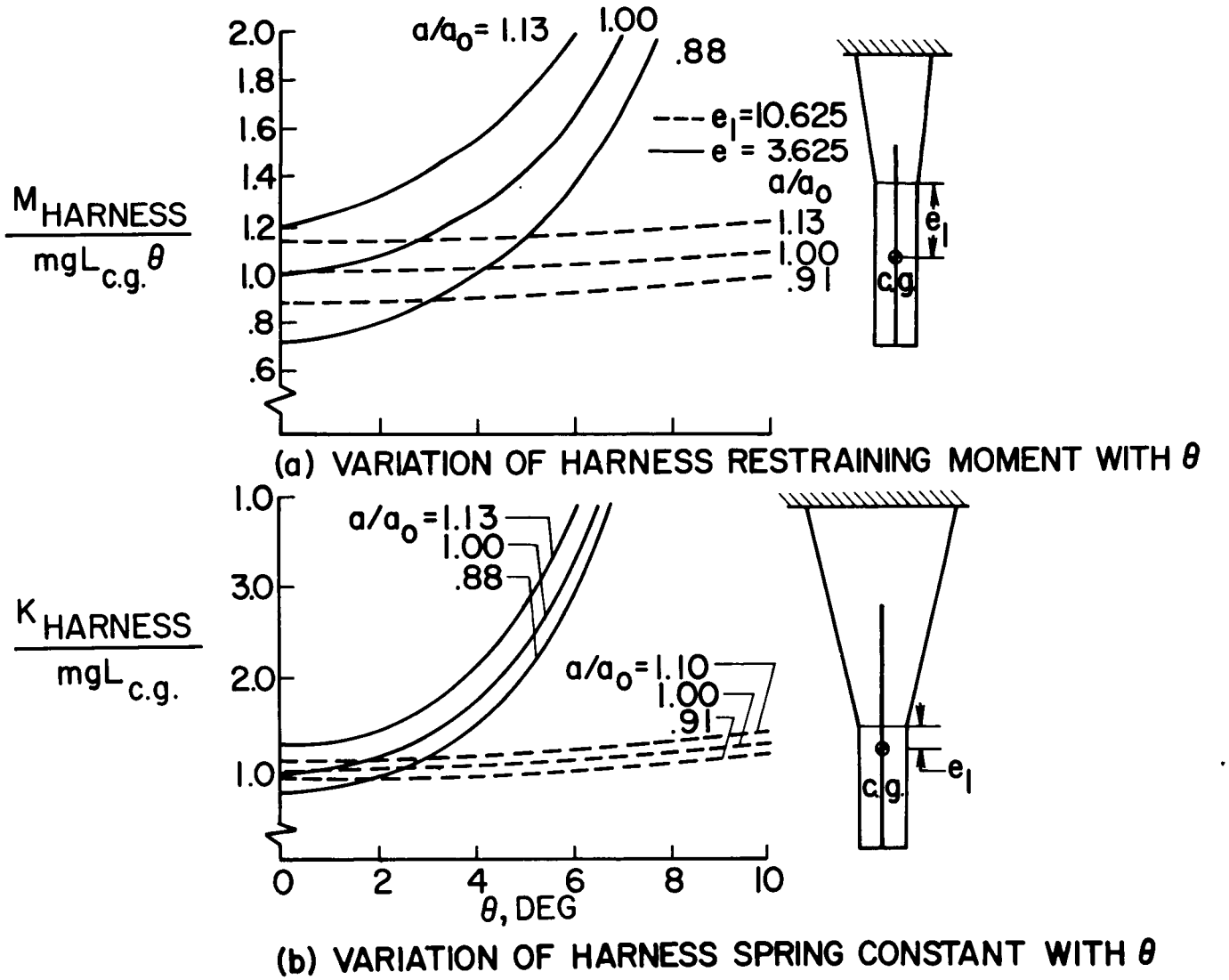

NASA

Figure 8.- Restraining moment and spring constant for two locations of restraining cables e_1. (eff) = 42.25 in.; (e - e_1) = 9.375; b = c = 4 in.; d = 0.

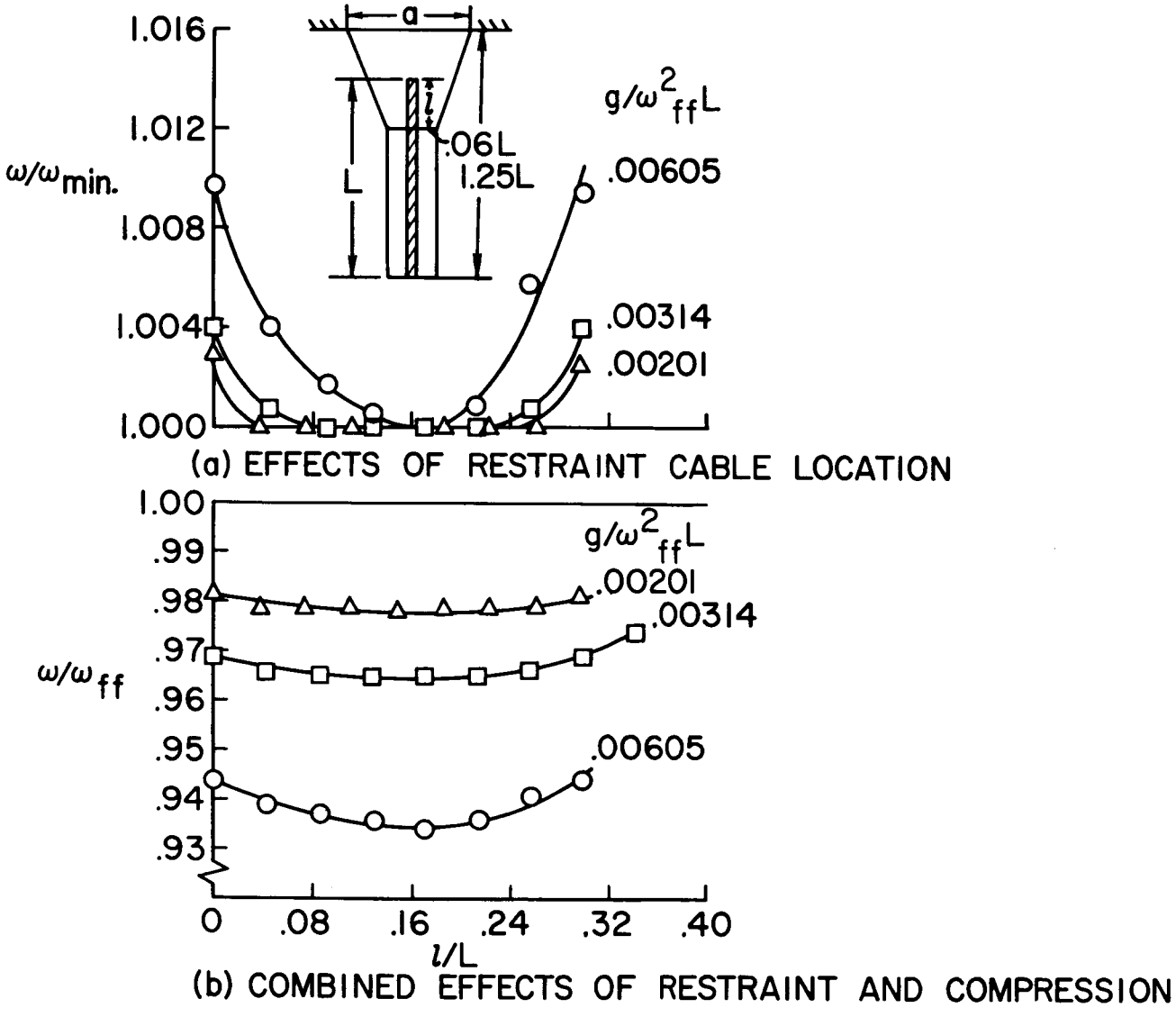

NASA

Figure 9.- Frequencies of uniform beams suspended in harness.

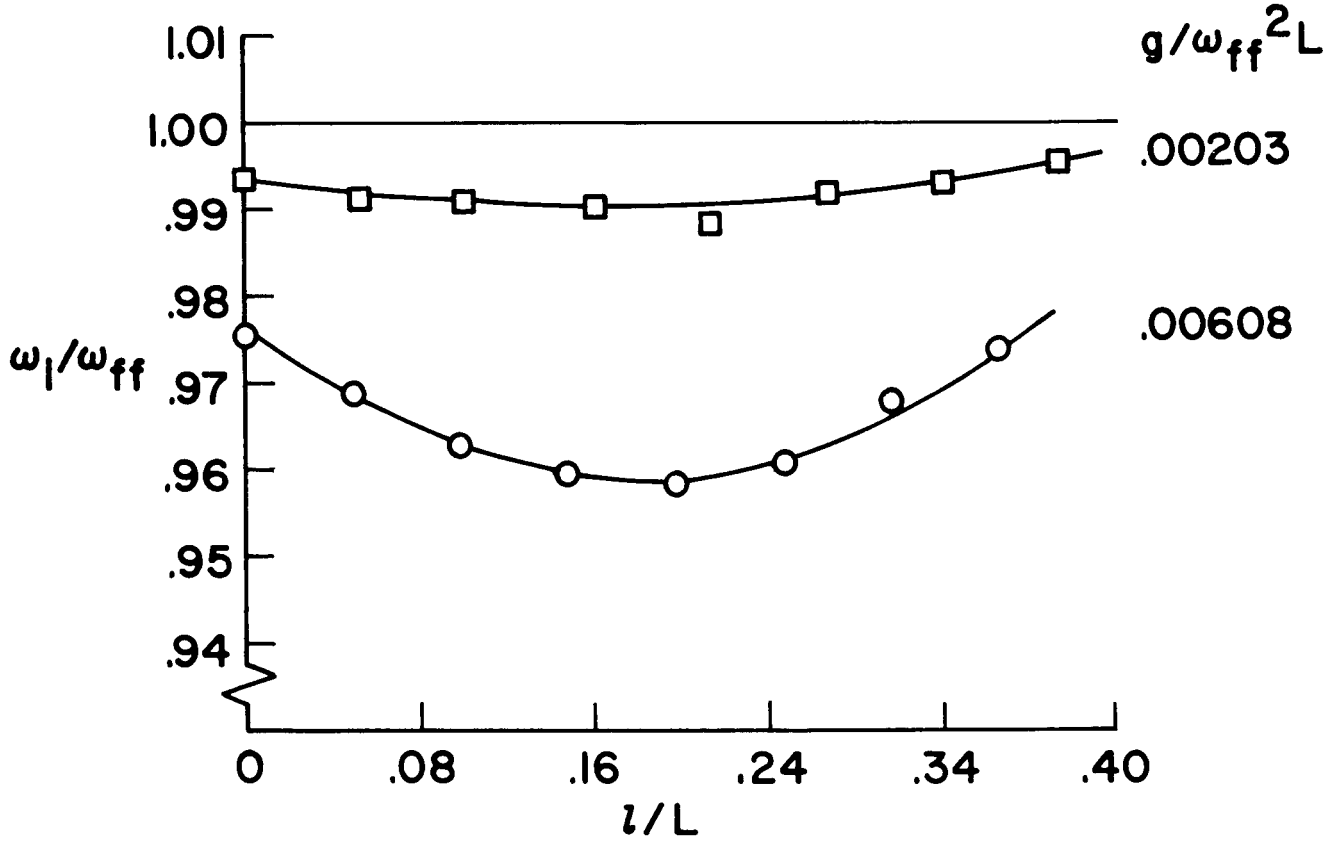

NASA

Figure 10.- Frequencies of nonuniform beams suspended in harness.

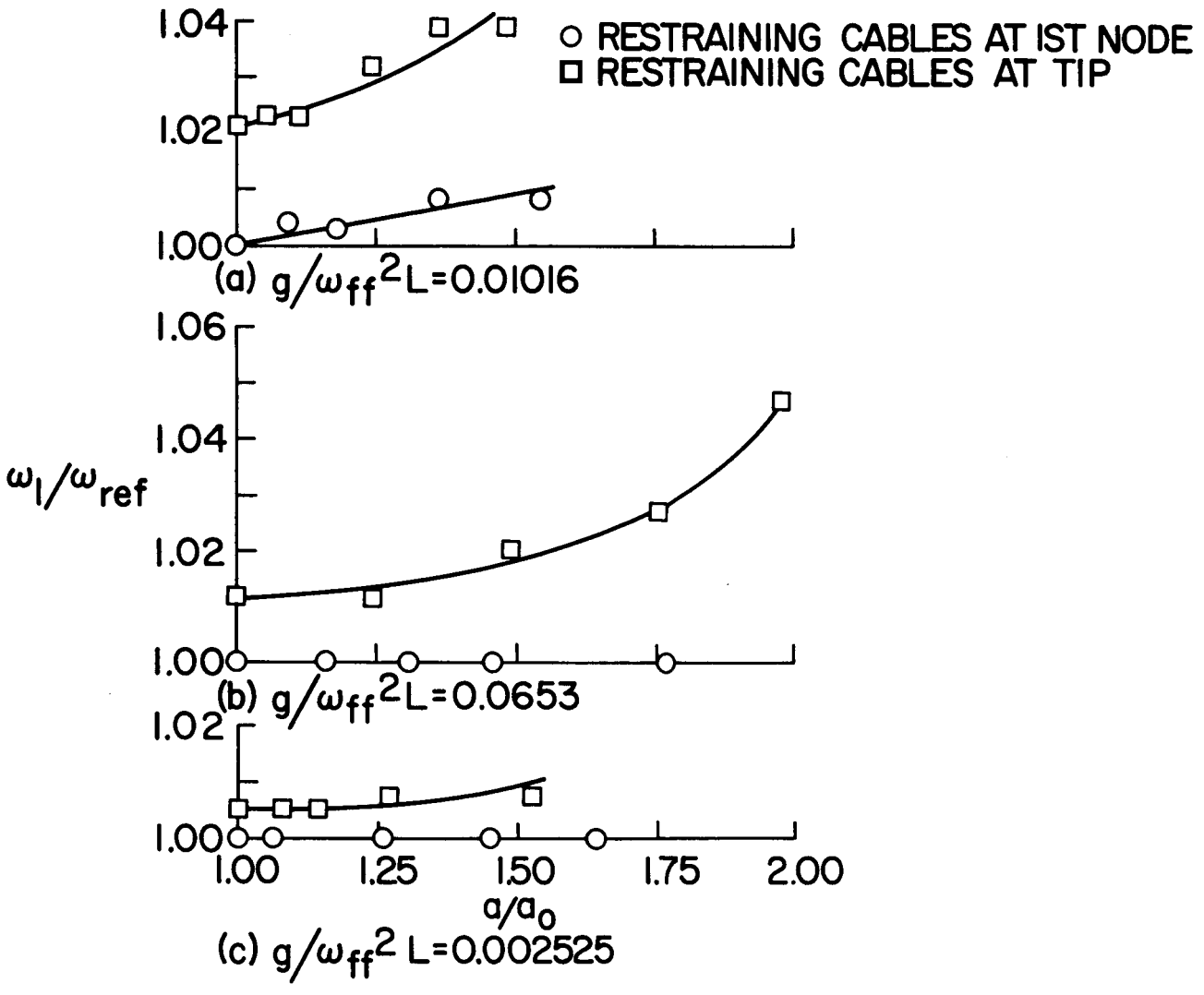

NASA

Figure 11.- Effects of using support-cable separation greater than optimum.

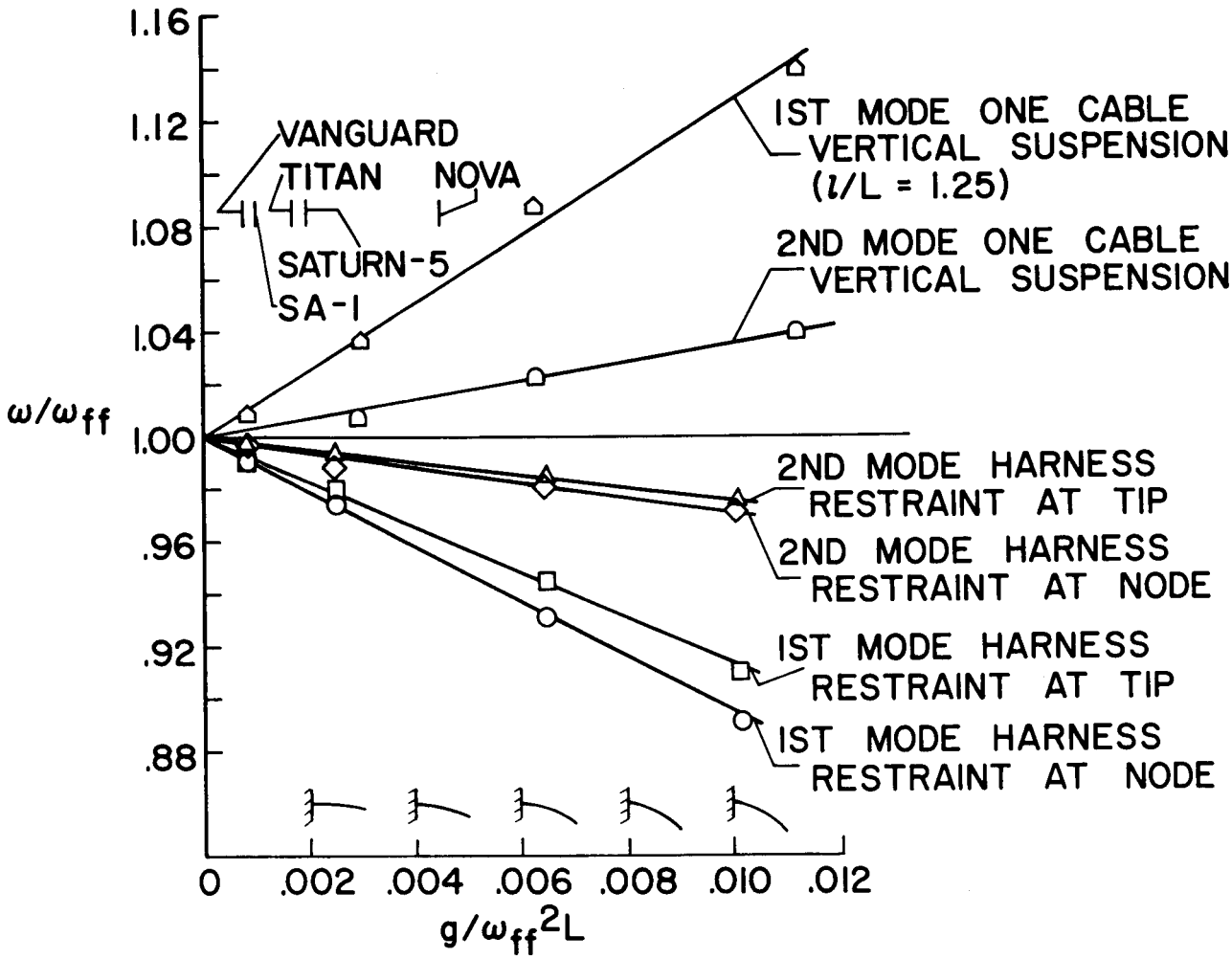

NASA

Figure 12.- Comparison of results obtained with one-cable vertical suspension and harness suspension.

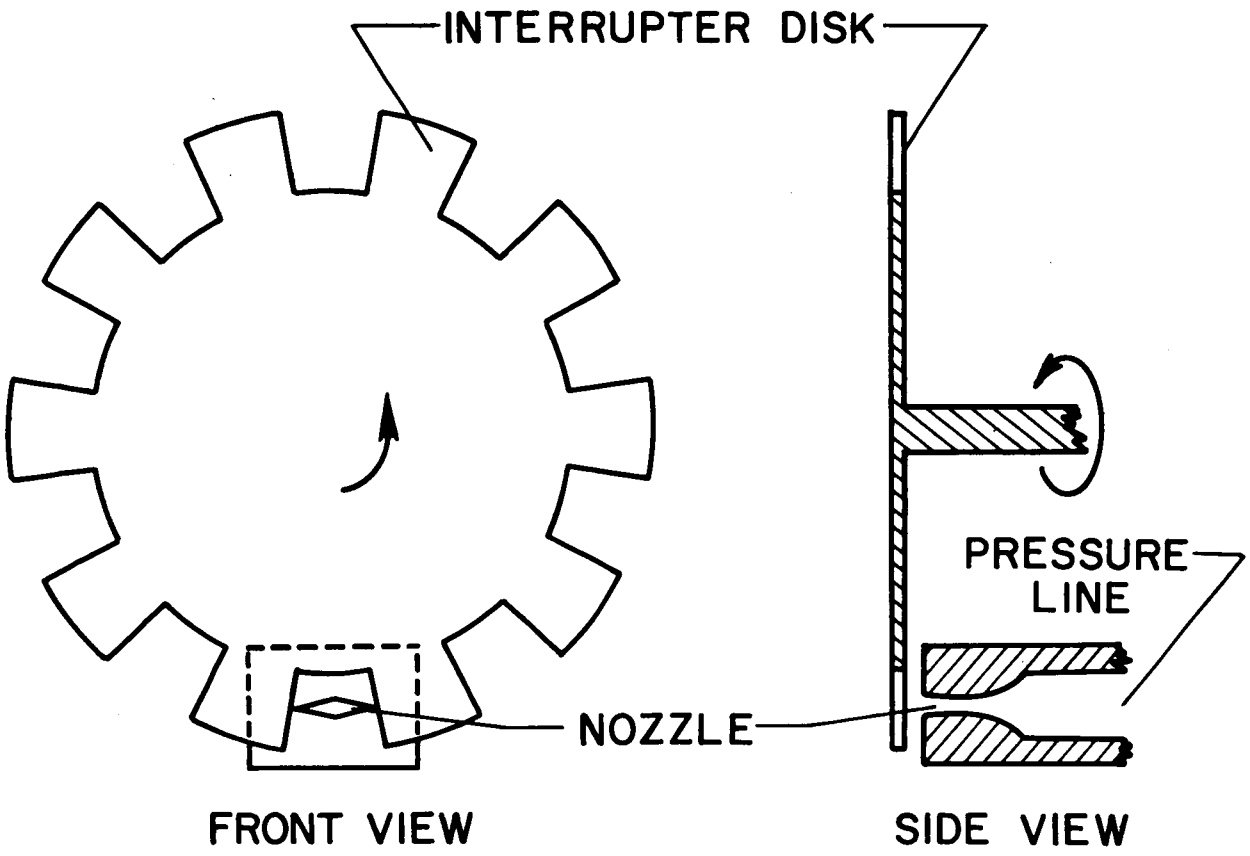

NASA

Figure 13.- Sketch of interrupter disk and nozzle.

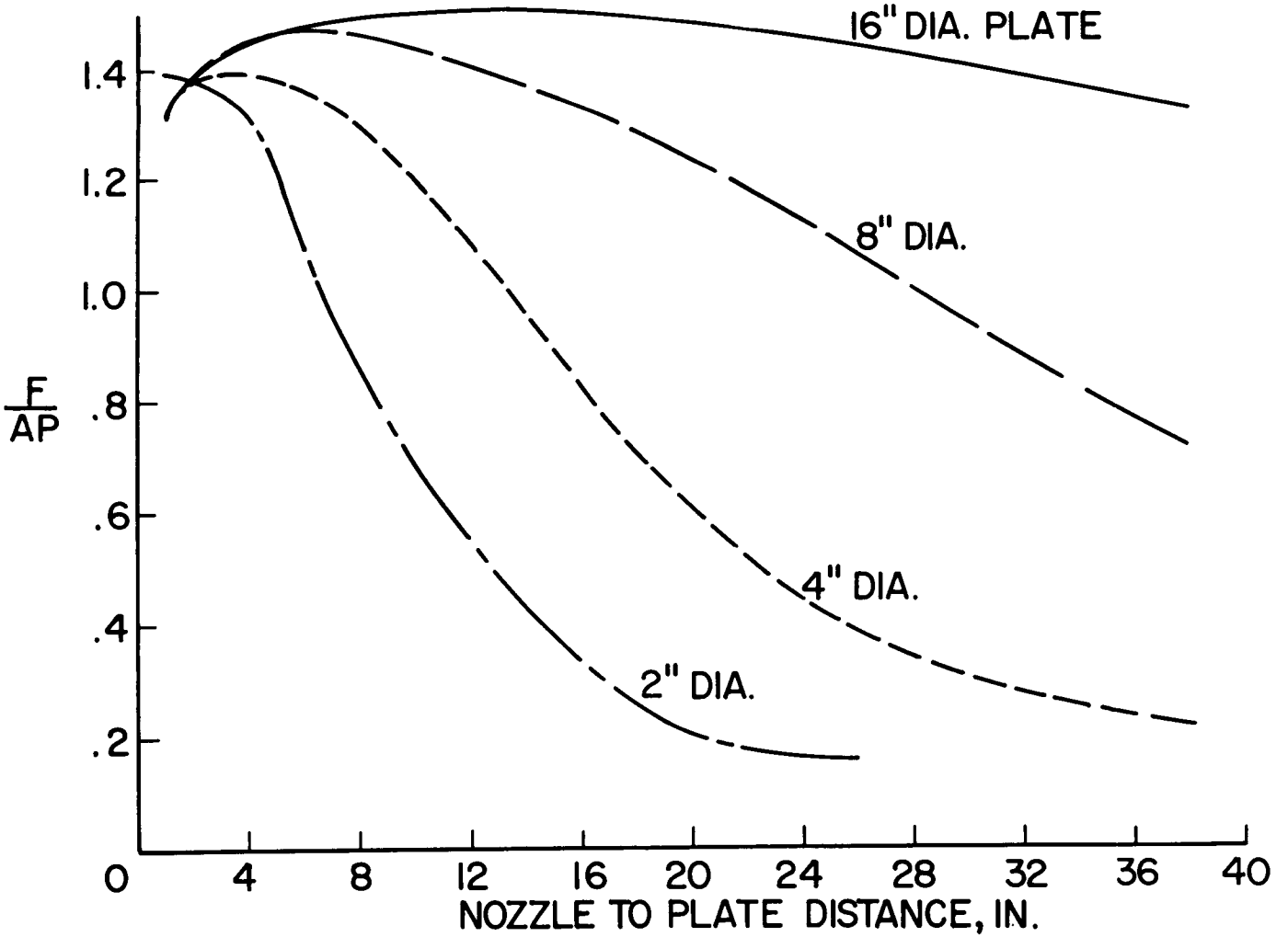

Figure 14.- Force coefficient as function of plate distance for various size plates.

NASA-Langley, 1963